PHYSICAL REVIEW D **93,** 115026 (2016)

Lepton flavor violating decay of SM-like Higgs boson in a radiative neutrino mass model

T. T. Thuc,[1,‡] L. T. Hue,[1,†] H. N. Long,[2,3,*] and T. Phong Nguyen[4,§]

[1]*Institute of Physics, Vietnam Academy of Science and Technology, 10 Dao Tan, Ba Dinh, Hanoi 100000, Vietnam*

[2]*Theoretical Particle Physics and Cosmology Research Group, Ton Duc Thang University, Ho Chi Minh City 700000, Vietnam*

[3]*Faculty of Applied Sciences, Ton Duc Thang University, Ho Chi Minh City 700000, Vietnam*

[4]*Department of Physics, Cantho University, 3/2 Street, Ninh Kieu, Cantho 900000, Vietnam*

(Received 13 April 2016; published 20 June 2016)

The lepton flavor violating decay of the Standard Model-like Higgs boson (LFVHD) is discussed in the framework of the radiative neutrino mass model built in [K. Nishiwaki, H. Okada, and Y. Orikasa, Phys. Rev. D **92**, 093013 (2015)]. The branching ratio (BR) of the LFVHD is shown to reach 10^{-5} in the most interesting region of the parameter space shown in [K. Nishiwaki, H. Okada, and Y. Orikasa, Phys. Rev. D **92**, 093013 (2015)]. The dominant contributions come from the singly charged Higgs mediations, namely, the coupling of $h_2^{\pm}$ with exotic neutrinos. Furthermore, if the doubly charged Higgs boson is heavy enough to allow the mass of $h_2^{\pm}$ around 1 TeV, the mentioned BR can reach 10^{-4}. In addition, we obtain that the large values of $\mathrm{Br}(h \to \mu\tau)$ lead to very small ones of $\mathrm{Br}(h \to e\tau)$, much smaller than the various sensitivities of current experiments.

DOI: 10.1103/PhysRevD.93.115026

I. INTRODUCTION

The confirmation of the existence of a scalar boson, known as the Standard Model (SM)-like Higgs boson, is the greatest early success of the LHC [1,2]. In addition, the LHC has reported recently some significant new physics beyond the SM, where the lepton flavor violating decay of the Standard Model-like Higgs boson (LFVHD) $h \to \mu\tau$ is one of the hottest subjects [3]. The upper bound $\mathrm{Br}(h^0 \to \mu\tau) < 1.5 \times 10^{-2}$ at 95% C.L. was announced by the CMS Collaboration, in agreement with 1.85×10^{-2} at 95% C.L. from the ATLAS Collaboration. More interestingly, CMS has indicated a 2σ excess of this decay, with the value of $\mathrm{Br}(h \to \mu\tau) = 0.84^{+0.39}_{-0.37}\%$. In addition, two other lepton flavor violating (LFV) decays of the SM-like Higgs boson have set experimental upper bounds at $\mathrm{BR}(h \to e\tau) < 0.7\%$ and $\mathrm{BR}(h \to e\mu) < 0.036\%$ at 95% C.L. [4]. Theoretically, many publications have studied how large $\mathrm{BR}(h \to \mu\tau)$ can become in specific models beyond the SM, such as the seesaw [5,6], supersymmetry (SUSY) [5,7], two Higgs doublet [8,9], and 3-3-1 models [10], as well as other interesting ones [11–13]. The LFV decay of new neutral Higgs bosons in non-SUSY models has also been discussed [14]. The significance of the LFVHD in colliders was addressed in [15].

The first source of LFV decays results from the mixing of different flavor massive neutrinos [16]. The simplest models explaining the mixing and the masses of active neutrinos may be the seesaw models, but the branching ratio (BR) of LFV decays predicted by these models are very small. Perhaps the inverse seesaw model gives the largest BR, which is about 10^{-5} [6]. All of the SUSY models, even the Minimal Supersymmetric Standard Model, easily predict large values of the BR of the LFVHD with new LFV sources in the slepton sector. However, the particle spectra of these models are rather complicated. In contrast, recent studies have shown that many of the non-SUSY models inheriting simpler particle spectra can predict very large BRs of the LFVHD at one-loop level, satisfying all relevant experimental constraints. Some of these models even have tree level couplings of the LFVHD, and they simultaneously explain other interesting experimental results [8].

There is another class of models, where neutrino mass is radiatively generated, that can predict large BRs of the LFVHD. These models do not have active neutrino mass terms at tree level, but they contain LFV couplings of new particles such as scalars and new leptons in order to generate neutrino masses from loop contributions. There is an interesting property that dictates that the loop suppression factors appearing in the expression of neutrino masses lead to the alleviation of the hierarchy in couplings. Hence, the aforementioned models will allow large Yukawa couplings, which may result in large BR values for many LFV processes. By investigating a specific model with three-loop

*Corresponding author.
hoangngoclong@tdt.edu.vn
†lthue@iop.vast.vn
‡ttthuc@grad.iop.vast.vn
§thanhphong@ctu.edu.vn

neutrino mass introduced in [17], we try to make clear how large the BR of the LFVHD can reach in the allowed regions. Furthermore, the contributions from active neutrino mediations may be enhanced because the Glashow-Iliopoulos-Maiani (GIM) mechanism does not work. Using the 't Hooft–Feynman gauge where loop contributions from private Feynman diagrams are all finite, we can compute and compare them. As a result, the best regions for large BRs of the LFVHD can be found with precise conditions of free parameters. The contributions from active neutrino mediations are divided completely into independent contributions of $W^{\pm}$ and new singly charged Higgs bosons. As we will see later, the active neutrino loops in the radiative neutrino mass model may give significant contributions to LFV processes. This is different from all of the other models, where these contributions are either ignored or are difficult to estimate when active neutrinos mix with new leptons, as in the case of the (inverse) seesaw models.

Our paper is arranged as follows. Section II will collect all needed ingredients for calculating the BR of the LFVHD. Section III concentrates on detailed expressions of the LFVHD amplitudes and partial widths. The constraints given in [17] will be discussed to find the allowed regions of parameter space. A numerical discussion is conducted and the main results are summarized in Secs. IV and V. Finally, the Appendixes A and B list analytic expressions of Passarino-Veltman (PV) functions and LFVHD form factors. The divergence cancellations of particular one-loop Feynman diagrams in the 't Hooft–Feynman gauge are proved in Appendix B.

II. REVIEW OF THE MODEL

A. Particle content

Following Ref. [17], the particle content of the model is listed in Table I, where the last row represents charges of an additional global symmetry, $U(1)$. Aside from the SM particles, new particles are all gauge singlets, including three Majorana fermions, $N_{R_{1,2,3}}$; one neutral Higgs boson, Σ_0; four singly charged Higgs bosons, $(h_1^{\pm}, h_2^{\pm})$; and two doubly charged Higgs bosons, $k^{\pm\pm}$. After the breaking of the $U(1)$ symmetry, a remnant Z_2 symmetry keeps $N_{R_{1,2,3}}$ and $h_2^{\pm}$ as negative parity particles. The remaining particles are trivial. An interesting consequence is that the lightest Majorana neutrino, which has negative parity, will be stable and can be a dark matter candidate.

The Yukawa sector $\mathcal{L}_Y$ respecting all mentioned symmetries is given as

$$-\mathcal{L}_Y = (y_\ell)_{ij}\overline{L'_{L_i}}\Phi e_{R_j} + \frac{1}{2}(y_L)_{ij}\overline{(L'_{L_i})^c}L'_{L_j}h_1^+ + (y_R)_{ij}\overline{N_{R_i}}(e_{R_j})^c h_2^- + \frac{1}{2}(y_N)_{ij}\Sigma_0\overline{(N_{R_i})^c}N_{R_j} + \text{H.c.} \tag{1}$$

In addition, when symmetries are broken, an effective Yukawa term appears after we take into account the loop contributions for generating active neutrino masses, namely,

$$-\mathcal{L}_Y^{\text{eff}} = \frac{(m_\nu)_{ab}}{\sqrt{2}v'} \times \overline{(\nu_{L_a})^c}\nu_{L_b} \times \Sigma_0, \tag{2}$$

corresponding to the active neutrino mass term derived in [17].

The Higgs potential is

$$\begin{aligned}\mathcal{V} = {} & m_\Phi^2|\Phi|^2 + m_\Sigma^2|\Sigma_0|^2 + m_{h_1}^2|h_1^+|^2 + m_{h_2}^2|h_2^+|^2 + m_k^2|k^{++}|^2 + [\lambda_{11}\Sigma_0^* h_1^- h_1^- k^{++} + \mu_{22}h_2^+h_2^+k^{--} + \text{H.c.}] + \lambda_\Phi|\Phi|^4 \\ & + \lambda_{\Phi\Sigma}|\Phi|^2|\Sigma_0|^2 + \lambda_{\Phi h_1}|\Phi|^2|h_1^+|^2 + \lambda_{\Phi h_2}|\Phi|^2|h_2^+|^2 + \lambda_{\Phi k}|\Phi|^2|k^{++}|^2 + \lambda_\Sigma|\Sigma_0|^4 + \lambda_{\Sigma h_1}|\Sigma_0|^2|h_1^+|^2 + \lambda_{\Sigma h_2}|\Sigma_0|^2|h_2^+|^2 \\ & + \lambda_{\Sigma k}|\Sigma_0|^2|k^{++}|^2 + \lambda_{h_1}|h_1^+|^4 + \lambda_{h_1h_2}|h_1^+|^2|h_2^+|^2 + \lambda_{h_1k}|h_1^+|^2|k^{++}|^2 + \lambda_{h_2}|h_2^+|^4 + \lambda_{h_2k}|h_2|^2|k^{++}|^2 + \lambda_k|k^{++}|^4.\end{aligned} \tag{3}$$

TABLE I. Lepton and scalar fields proposed in [17]. The notations L'_{L_i} and ν'_{L_i} denote the flavor states, in contrast to the mass state ν_{L_i} used later.

Characters	Lepton fields			Scalar fields				
	$L'_{L_i} = \binom{\nu'_{L_i}}{e_{L_i}}$	e_{R_i}	N_{R_i}	Φ	Σ_0	h_1^+	h_2^+	k^{++}
$SU(3)_C$	**1**	**1**	**1**	**1**	**1**	**1**	**1**	**1**
$SU(2)_L$	**2**	**1**	**1**	**2**	**1**	**1**	**1**	**1**
$U(1)_Y$	$-1/2$	-1	0	$1/2$	0	1	1	2
$U(1)$	0	0	$-x$	0	$2x$	0	x	$2x$

The scalar fields are parametrized as

$$\Phi = \begin{pmatrix} G_w^+ \\ \frac{v+\phi+iG_z}{\sqrt{2}} \end{pmatrix}, \qquad \Sigma_0 = \frac{v'+\sigma}{\sqrt{2}}e^{iG/v'}, \tag{4}$$

where $v \simeq 246$ GeV, v' is a new vacuum expectation value (VEV), and $G_w^{\pm}$ and G_Z are Goldstone bosons of $W^{\pm}$ and Z bosons, respectively.

The above lepton and Higgs sectors show that the singly charged Higgs bosons contribute mainly to the BR of the

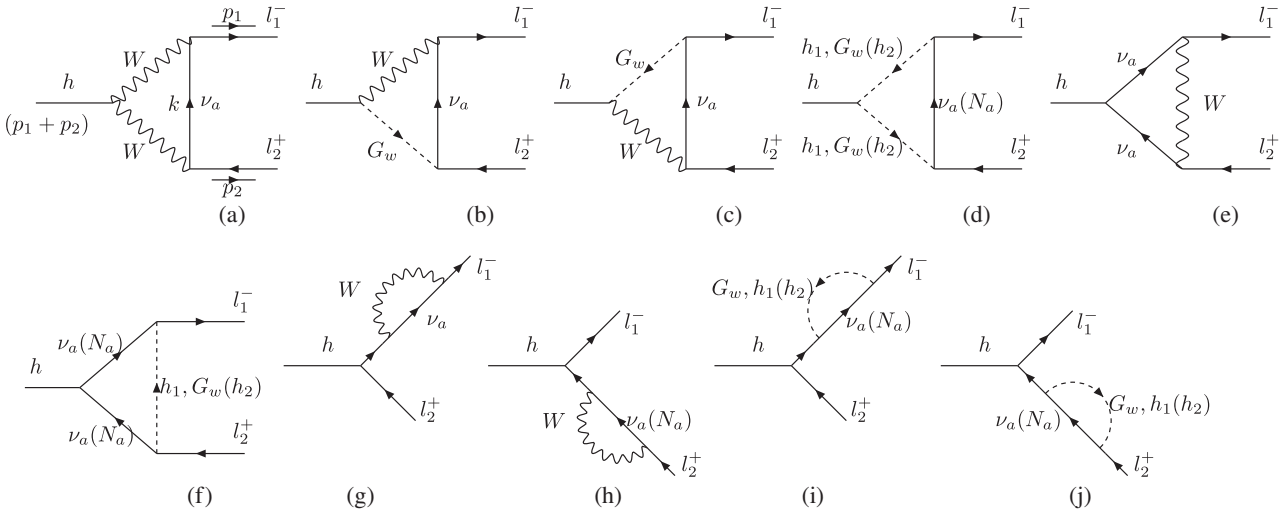

FIG. 1. Feynman diagrams for the LFVHD $h \to \mu^{\pm}\tau^{\mp}$ decay, where h, $l_1 \equiv e_2 = \mu$, $l_2 \equiv e_3 = \tau$. The parentheses imply that N_a and $h_2^{\pm}$ couple with each other only.

LFVHD, while the doubly charged Higgs bosons do not. Because all of the charged Higgs bosons are $SU(2)_L$ singlets, they do not couple with W bosons like new Higgs multiplets in other models. At the one-loop level and 't Hooft–Feynman gauge, the Feynman diagrams for the LFVHD are shown in Fig. 1.

In order to investigate the LFVHD, the amplitudes will be calculated using the 't Hooft–Feynman gauge. The amplitudes are formulated as functions of the PV functions analyzed in [10]. The notations of four-component (Dirac) spinors are used for leptons. Specifically, the charged leptons are e_i, so that the left-handed component is $e_{L_i} = P_L e_i$ and the right-handed one is $e_{R_i} = P_R e_i$, where $P_{R,L} \equiv (1 \pm \gamma_5)/2$ are chiral operators. The corresponding charge conjugations are $e_i^c \equiv C\overline{e_i}^T = (e_{L_i}^c, e_{R_i}^c)^T$, which satisfies $e_{L_i}^c = P_L e_i^c = C\overline{e_{R_i}}^T \equiv (e_{R_i})^c$ and $e_{R_i}^c = P_R e_i^c = C\overline{e_{L_i}}^T \equiv (e_{L_i})^c$. For the Majorana leptons such as active and exotic neutrinos, the four-spinors are $\nu_i' = \nu_i'^c = (\nu_{L_i}', (\nu_{L_i}')^c)^T = (\nu_{L_i}', \nu_{R_i}'^c)^T$ and $N_i = N_i^c = ((N_{R_i})^c, N_{R_i})^T = (N_{L_i}^c, N_{R_i})^T$. To reduce the second and third terms of (1) to more convenient forms, we will use equalities like $\overline{e_i^c} P_L \nu_j' = \overline{\nu_j'^c} P_L e_i = \overline{\nu_j'} P_L e_i$ and $\overline{N_{R_i}}(e_{R_j})^c = \overline{N_i} P_L e_j^c = \overline{e_j} P_L N_i^c = \overline{e_j} P_L N_i$ (Appendix G of [18]).

B. Mass spectrum and LFVHD couplings

In the mass basis, the model consists of two CP-even neutral Higgs bosons; a Nambu-Goldstone scalar boson G; four singly charged Higgs bosons, $h_1^{\pm}$, $h_2^{\pm}$; and two doubly charged Higgs bosons, $k^{\pm\pm}$. At one-loop level, the LFVHD involves only two CP-even neutral and four singly charged Higgs bosons. The two CP-even neutral Higgs bosons are a SM-like Higgs boson, h ($m_h = 125$ GeV) and a new CP-even one, H. They relate to the original Higgs components (ϕ, σ) via the transformation

$$\begin{pmatrix} \phi \\ \sigma \end{pmatrix} = \begin{pmatrix} c_\alpha & s_\alpha \\ -s_\alpha & c_\alpha \end{pmatrix} \begin{pmatrix} h \\ H \end{pmatrix}, \tag{5}$$

where $c_\alpha \equiv \cos\alpha$, $s_\alpha \equiv \sin\alpha$, and α is defined as

$$\sin 2\alpha = \frac{2\lambda_{\Phi\Sigma} v v'}{m_H^2 - m_h^2}. \tag{6}$$

The masses m_h and m_H are functions of the four parameters λ_Φ, λ_Σ, $\lambda_{\Phi\Sigma}$, and v'. In the following calculations, we will fix $m_h = 125.1$ GeV, while m_H, s_α, and v' are taken as free parameters. The original parameters are given as [17]

$$\lambda_{\Phi\Sigma} = \frac{s_\alpha c_\alpha (m_H^2 - m_h^2)}{v v'}, \qquad \lambda_\Phi = \frac{c_\alpha^2 m_h^2 + s_\alpha m_H^2)}{2v^2},$$
$$\text{and} \quad \lambda_\Sigma = \frac{s_\alpha^2 m_h^2 + c_\alpha^2 m_H^2}{2v'^2}. \tag{7}$$

The perturbativity limit forces λ_Φ, λ_Σ, $\lambda_{\Phi\Sigma} \le 4\pi$ and therefore gives an upper bound on m_H with a large s_α. For example, $|s_\alpha| \le 0.3$ corresponds to $m_H \le 4$ TeV.

The masses of the singly charged Higgs bosons are given as

$$m_{h_1^{\pm}}^2 = m_{h_1}^2 + \frac{1}{2}(\lambda_{\Phi h_1} v^2 + \lambda_{\Sigma h_1} v'^2),$$
$$m_{h_2^{\pm}}^2 = m_{h_2}^2 + \frac{1}{2}(\lambda_{\Phi h_2} v^2 + \lambda_{\Sigma h_2} v'^2). \tag{8}$$

Regarding the lepton sector, the first and last terms in (1) correspond to the mass terms of charged leptons and exotic neutrinos, respectively. They are assumed to be diagonal, i.e., the flavor basis and the mass basis coincide. Their expressions are obtained as

$$m_{e_i} = (y_\ell)_{ii} \frac{v}{\sqrt{2}}, \qquad m_{N_i} = \frac{v'}{\sqrt{2}} (y_N)_{ii}. \tag{9}$$

The active neutrino masses generated from three-loop corrections can be expressed by the effective term (2). The components of active neutrino mass matrix are given as [17]

$$(m_\nu)_{ab} = \frac{\mu_{11}\mu_{22}}{(4\pi)^6}\sum_{i,j,k=1}^{3}\frac{1}{M_k^4} \times [(y_L)_{ai} m_{e_i} (y_R^T)_{ik} (M_{N_k}) (y_R)_{kj} m_{e_j} (y_L^T)_{jb}] \times F_1\left(\frac{m_{h_1^+}^2}{M_k^2}, \frac{m_{h_2^+}^2}{M_k^2}, \frac{m_{\ell_i}^2}{M_k^2}, \frac{m_{\ell_j}^2}{M_k^2}, \frac{M_{N_k}{}^2}{M_k^2}, \frac{m_{k^{\pm\pm}}^2}{M_k^2}\right), \quad (10)$$

where M_k is the maximal value among the quantities $m_{h_1^\pm}$, $m_{h_2^\pm}$, m_{e_i}, m_{e_j}, M_{N_k}, $m_{k^{\pm\pm}}$; $\mu_{11} \equiv \lambda_{11} v'/\sqrt{2}$; and F_1 is the three-loop function given in detail in [17].

All of the mass terms—together with the couplings $h\bar{f}f$, where $f = e_i$, ν_i, and N_i—are parts of Yukawa terms of neutral Higgs bosons. The flavor states ν'_{L_i} and mass states ν_{L_i} $(i = 1, 2, 3)$ of active neutrinos are related by the transformation $\nu'_{L_i} = U^L_{ij}\nu_{L_j}$, where $U^L U^{L\dagger} = U^{L\dagger} U^L = 1$. The masses and mixing angles of the active neutrinos are taken from the best-fit experimental data given in [19]. The only unknown parameter is the lightest mass.

Concentrating only on the mass terms and couplings involving the LFVHD of the SM-like Higgs boson, the Yukawa interactions (1) and (2) are written as follows:

$$\begin{aligned}-\mathcal{L}'_Y = {} & m_{e_i}\overline{e_i}e_i + \frac{1}{2}m_{\nu_i}\overline{\nu_i}\nu_i + \frac{1}{2}m_{N_i}\overline{N_i}N_i + \frac{m_{e_i}}{v}\overline{e_i}e_i(c_\alpha h) \\ & - \left[\frac{m_{N_i}}{2v'}\overline{N_i}N_i + \frac{m_{\nu_i}}{2v'}\overline{\nu_i}\nu_i\right]s_\alpha h + \frac{\sqrt{2}m_{e_i}}{v}[U^L_{ij}\overline{e_i}P_L\nu_j G_w^- \\ & + U^{L*}_{ij}\overline{\nu_j}P_R e_i G_w^+] + (y_L^T U^{L*})_{ij}\overline{\nu_j}P_L e_i h_1^+ \\ & + (y_L^T U^L)_{ij}\overline{e_i}P_R\nu_j h_1^- + (y_R^T)_{ij}\overline{e_i}P_L N_j h_2^- \\ & + (y_R^T)_{ij}\overline{N_j}P_R e_i h_2^+. \end{aligned} \quad (11)$$

The LFV couplings relating to the $W^\pm$ gauge boson only occur in the covariant kinetic terms of $SU(2)_L$ doublets, exactly the same as in the SM, namely,

$$\mathcal{L}^l_{\text{kin}} = i\overline{L_{L_i}}\gamma^\mu D_\mu L_{L_i} + (D_\mu\Phi)^\dagger(D^\mu\Phi), \quad (12)$$

where D_μ is the covariant derivative defined in the SM. All relevant couplings of the LFVHD are collected in Table II.

C. Parameter constraints from the previous work

For calculating the BR of the LFVHD, in the following sections we will mainly use the constraints of parameters obtained in [17]. The important points are reviewed as follows. The parameters in the model were first investigated to ensure that they satisfy the neutrino oscillation data, the current bounds of the BR of the LFV processes, the universality of the charged currents, and the vacuum stability of the Higgs self-couplings. In addition, the doubly charged Higgs bosons $k^{\pm\pm}$ are assumed to be light enough that they could be detected at the LHC. The constraints on parameters involved with the LFVHD are (i) the Dirac phase of the active neutrino mixing matrix prefers the value of $\delta = \pi$, while the Majorana phase is still free; (ii) the masses of singly charged Higgs bosons should not be smaller than 3 TeV; (iii) the value of $|(y_R)_{22}|$ should be around 9; (iv) the value of v' should be on the order of $O(1)$ TeV. The investigation in [17] also showed that the heavier doubly charged Higgs bosons, $k^{\pm\pm}$, will allow the lighter singly charged Higgs bosons. This leads to an interesting consequence of large values of the BR of the LFVHD, as we will show in the numerical investigation.

The constraint from the LHC Higgs boson search was also discussed in [17], including the effects of the $U(1)$ global Goldstone boson in the invisible decay of the SM-like Higgs boson and the pair annihilation of the dark matter (DM) candidate N_{R_1}. From this, the constraint of the mixing angle of neutral Higgs bosons is obtained as

TABLE II. Couplings of the LFVHD in the 't Hooft–Feynman gauge. The momenta are incoming.

Vertex	Coupling	Vertex	Coupling
$h\overline{e_i}e_i$	$-\frac{im_{e_i}}{v}c_\alpha$	$h\overline{\nu_i}\nu_i$	$\frac{im_{\nu_i}}{v'}s_\alpha$
$h\overline{N_i}N_i$	$\frac{im_{N_i}}{v'}s_\alpha$	$hW_\mu^+W_\nu^-$	$igm_W c_\alpha g^{\mu\nu}$
$hh_1^+h_1^-$	$i(-vc_\alpha\lambda_{\Phi h_1} + v's_\alpha\lambda_{\Sigma h_1})$	$hh_2^+h_2^-$	$i(-vc_\alpha\lambda_{\Phi h_2} + v's_\alpha\lambda_{\Sigma h_2})$
$h(p_0)W_\mu^+G_w^-(p_-)$	$\frac{ig}{2}c_\alpha(p_0 - p_-)^\mu$	$h(p_0)W_\mu^-G_w^+(p_+)$	$-\frac{ig}{2}c_\alpha(p_0 - p_+)^\mu$
$\overline{e_i}\nu_j h_1^-$	$-i(y_L^T U^L)_{ij}P_R$	$\overline{\nu_j}e_i h_1^+$	$i(y_L^T U^L)^*_{ij}P_L$
$\overline{e_i}\nu_j G_w^-$	$-i\frac{\sqrt{2}m_{e_i}}{v}U^L_{ij}P_L$	$\overline{\nu_j}e_i G_w^+$	$-i\frac{\sqrt{2}m_{e_i}}{v}U^{L*}_{ij}P_R$
$\overline{e_i}N_j h_2^-$	$-i(y_R^T)_{ij}P_L$	$\overline{N_j}e_i h_2^+$	$-i(y_R^T)_{ij}P_R$
$\overline{e_i}\nu_j W_\mu^-$	$\frac{ig}{\sqrt{2}}U^L_{ij}\gamma^\mu P_L$	$\overline{\nu_j}e_i W_\mu^+$	$\frac{ig}{\sqrt{2}}U^{L*}_{ij}\gamma^\mu P_L$
$hG_w^+G_w^-$	$i(-2vc_\alpha\lambda_\Phi + v's_\alpha\lambda_{\Phi\Sigma})$		

$|\sin\alpha| \leq 0.3$. Finally, the condition of the DM candidate mentioned above leads to the conclusion that the N_{R_1} mass should be around the value of $m_h/2$ in order to successfully explain the current relic density of DM; the VEV v' was found to be smaller than 10 TeV.

Many other issues involved with the global $U(1)$ Goldstone boson were discussed in detail in [17], for instance, anomaly induced interaction to two photons, active-sterile neutral lepton mixing, and neutrinoless double beta decay via W exchange. Possible bounds from cosmological issues, such as the effect on the cosmic microwave background via the cosmic string generated by the spontaneous breaking down of the global $U(1)$ symmetry, were also mentioned. None of these issues change the constraints of the parameters indicated above. Though new constraints on DM masses in the presence of $U(1)$ global symmetry were addressed in [20], more studies are needed for confirmation. Furthermore, the considered global symmetry can be moved straight to the local one [17], or replaced with a suitable discrete symmetry. That discussion is beyond the scope of this work.

In the next section, we will focus on parameters affecting the LFVHD and will discuss more clearly the relevant constraints, if ones are needed.

III. FORMULAS OF THE LFVHD AND PARAMETER CONSTRAINTS

The effective Lagrangian of the decay $h \to \tau^{\pm}\mu^{\mp}$ is written as $\mathcal{L}^{\rm LFV} = h(\Delta_L \bar{\mu} P_L \tau + \Delta_R \bar{\mu} P_R \tau) + \text{H.c.}$, where $\Delta_{L,R}$ are scalar factors arising from the loop contributions. The decay amplitude is defined as $i\mathcal{M} = i\bar{u}_1(\Delta_L P_L + \Delta_R P_R)v_2$ [6], where $u_1 \equiv u_1(p_1, s_1)$ and $v_2 \equiv v_2(p_2, s_2)$ are the Dirac spinors of a muon and a tauon, respectively. The partial width of the decay is given as

$$\Gamma(h \to \mu\tau) \equiv \Gamma(h \to \mu^-\tau^+) + \Gamma(h \to \mu^+\tau^-) = \frac{m_h}{8\pi}(|\Delta_L|^2 + |\Delta_R|^2), \tag{13}$$

with the condition $m_h \gg m_1, m_2$, where m_1, m_2 are muon and tauon masses, respectively. The on-shell conditions for external particles are $p_i^2 = m_i^2$ $(i = 1, 2)$ and $p_h^2 \equiv (p_1 + p_2)^2 = m_h^2$.

The loop contributions can be separated into two parts, $\Delta_L = \Delta_L^{\nu} + \Delta_L^N$ and $\Delta_R = \Delta_R^{\nu} + \Delta_R^N$, corresponding to the appearance of the active and exotic neutrinos in the loops. In the 't Hooft–Feynman gauge, the specific formulas of contributions from the diagrams shown in Fig. 1 are listed in Appendix B, where new notations such as $E_{L,R}$ factors are used. The contribution of the loops with active neutrinos Δ_L^{ν} is obtained as

$$\begin{aligned}\Delta_L^{\nu} = \frac{1}{16\pi^2}\sum_{a=1}^{3}(y_L^T U^L)_{2a}(y_L^T U^L)^*_{3a}\Big[(v'\lambda_{hh_1h_1})E_L^{\nu h_1 h_1} \\ + s_\alpha E_L^{h_1\nu\nu} + (-c_\alpha)E_L^{h_1\nu}\Big] + \frac{1}{16\pi^2}\sum_{a=1}^{3} U_{2a}^L U_{3a}^{L*} \\ \times\Bigg[g^3 c_\alpha E_L^{\nu WW} + \frac{g^2 c_\alpha}{2}(E_L^{\nu G_w W} + E_L^{\nu W G_w}) \\ + (v'\lambda_{hG_wGw})E_L^{\nu G_w G w} + s_\alpha\left(\frac{g^2}{2}E_L^{W\nu\nu} + E_L^{G_w\nu\nu}\right) \\ - c_\alpha\left(\frac{g^2}{2}E_L^{W\nu} + E_L^{G_w\nu}\right)\Bigg],\end{aligned} \tag{14}$$

where $(v'\lambda_{hh_1h_1}) = -vc_\alpha\lambda_{\Phi h_1} + v's_\alpha\lambda_{\Sigma h_1}$ and $(v'\lambda_{hG_wGw}) = -2vc_\alpha\lambda_\Phi + v's_\alpha\lambda_{\Phi\Sigma}$.

The contribution from the exotic neutrino mediations Δ_L^N is given as

$$\begin{aligned}\Delta_L^N = \frac{1}{16\pi^2}\sum_{a=1}^{3}(y_R^T)_{2a}(y_R^T)_{3a}\Big[(v'\lambda_{hh_2h_2})E_L^{Nh_2h_2} \\ + s_\alpha E_L^{h_2NN} - c_\alpha E_L^{Nh_2}\Big],\end{aligned} \tag{15}$$

where $(v'\lambda_{hh_2h_2}) = -vc_\alpha\lambda_{\Phi h_2} + v's_\alpha\lambda_{\Sigma h_2}$.

Similarly, we have $\Delta_R^{\nu} = \Delta_L^{\nu}(E_L \to E_R)$ and $\Delta_R^N = \Delta_L^N(E_L \to E_R)$.

As proved in Appendix B, the $\Delta_{L,R}$ are convergent. Specifically, in the 't Hooft–Feynman gauge, the private contributions from specific diagrams are always finite. In addition, the limit p_1^2, $p_2^2 \simeq 0$ results from the extremely small contributions of the diagrams related to the two point functions, namely, Figs. 1(g), 1(h), 1(i), and 1(j). Hence, their contributions are ignored. Besides, it can be estimated that the sum of the contributions in the two last lines in (14) is very suppressed because of the GIM mechanism, controlled by the factor $\sum_{a=1}^{3} U_{2a}^L U_{3a}^{L*}$. This is a general property of all models where the neutrino masses are generated from the seesaw mechanism. While the contributions of the first lines of (14) and (15) may be large because the appearance of y_L and y_R breaks the GIM mechanism, nonzero contributions survive which do not contain factors of very light neutrino masses.

In the numerical calculation, the following parameters are taken from experimental data, for example, [21]: $v \simeq 246$ GeV, $m_h = 125.1$ GeV, $m_W = 80.4$ GeV, and the muon and tauon masses are $m_\mu = 0.105$ GeV, $m_\tau = 1.776$ GeV. The total decay width of the SM-like Higgs boson $\Gamma_h = 4.1 \times 10^{-3}$ GeV is used. Based on the investigation of [17], relevant parameters of the active neutrino masses are only considered in the normal hierarchy scheme. For example, the mixing parameters U^L are expressed as follows:

$$U^L = \begin{pmatrix} 1 & 0 & 0 \\ 0 & c_{23} & s_{23} \\ 0 & -s_{23} & c_{23} \end{pmatrix} \begin{pmatrix} c_{13} & 0 & -s_{13} \\ 0 & 1 & 0 \\ s_{13} & 0 & c_{13} \end{pmatrix} \times \begin{pmatrix} c_{12} & s_{12} & 0 \\ -s_{12} & c_{12} & 0 \\ 0 & 0 & 1 \end{pmatrix}, \quad (16)$$

where $c_{ij} \equiv \cos\theta_{ij}$, $s_{ij} \equiv \sin\theta_{ij}$ and the Dirac CP phase δ and the Majorana CP phase ϕ are taken as $\delta = \pi$ and $\phi = 0$. The best-fit values of the neutrino oscillation parameters given in [19]

$$\Delta m^2_{21} = 7.50 \times 10^{-5}\ \text{eV}^2, \quad \Delta m^2_{31} = 2.457 \times 10^{-3}\ \text{eV}^2, \quad s^2_{12} = 0.304, \quad s^2_{23} = 0.452, \quad s^2_{13} = 0.0218 \quad (17)$$

are also used in our numerical calculations. The lightest neutrino mass will be chosen as $m_{\nu_1} = 10^{-10}$ GeV, satisfying the condition $\sum_b m_{\nu_b} \leq 0.5$ eV obtained from the cosmological constraint. The remain two neutrino masses are $m^2_{\nu_b} = m^2_{\nu_1} + \Delta m^2_{\nu_{b1}}$, where $b = 2, 3$.

The other unknown parameters involving the LFVHD are the VEV v'; the mixing angle of the two neutral Higgs bosons α; the exotic neutrino masses m_{N_a}; the new Higgs masses $m_{h^\pm_1}$, $m_{h^\pm_2}$, m_H; the Yukawa coupling matrices y_L and y_R; and the trilinear Higgs self-couplings $\lambda_{\Phi h_1}$, $\lambda_{\Phi h_2}$, $\lambda_{\Sigma h_1}$, $\lambda_{\Sigma h_2}$.

In the numerical investigation, we focus first on the most interesting regions of the parameter space indicated in [17], where m_{N_1} plays the role of a dark matter particle and the doubly charged Higgs bosons $k^{\pm\pm}$ are light enough to be observed at the LHC. The values of the relevant parameters are summarized as follows: $m_h/2 = m_{N_1} < m_{N_2} < m_{N_3}$, $|s_\alpha| \leq 0.3$; $3\ \text{TeV} \leq (m_{h^\pm_1}, m_{h^\pm_2}) \sim \mathcal{O}(1)$ TeV; and $v' \sim \mathcal{O}(1)$ TeV. The matrix Yukawa coupling matrix y_L satisfies the following conditions [22]:

$$(y_L)_{13} = \left(\frac{s_{12}c_{23}}{c_{12}c_{13}} - \frac{s_{13}s_{23}}{c_{13}}\right)(y_L)_{23} = 0.394(y_L)_{23},$$
$$(y_L)_{12} = \left(\frac{s_{12}s_{23}}{c_{12}c_{13}} + \frac{s_{13}c_{23}}{c_{13}}\right)(y_L)_{23} = 0.56(y_L)_{23}, \quad (18)$$

and $|(y_L)_{23}| \leq 1$. The conditions of gauge coupling universalities also imply that

$$|(y_L)_{23}| < \frac{0.3 m_{h^\pm_1}}{1\ \text{TeV}}. \quad (19)$$

The most stringent constraint comes from the LFV decay of a muon with $\text{Br}(\mu \to e\gamma) < 5.7 \times 10^{-13}$. It gives the direct upper bounds on the following products of the Yukawa couplings: (i) $(y^T_L)_{23}(y^T_L)_{13}$ in the loop including virtual active neutrinos and $h^\pm_1$ since y_L is antisymmetric, and (ii) $(y^T_R)_{2i}(y^T_R)_{1i}$ $(i = 1, 2, 3)$ in the loops including exotic neutrinos and $h^\pm_2$. The other constraints from the tauon decays are less stringent and hence are omitted here. On the other hand, $\text{Br}(h \to \mu\tau)$ depends on the products $(y^T_R)_{2i}(y^T_R)_{3i}$, with $i = 1, 2, 3$. So, if $|(y^T_R)_{ij}|$ with $(ij) = \{(11), (21), (31)\}$ is small enough, the values of $(y^T_R)_{ij}$ with $(ij) = \{(22), (32), (33)\}$ may be large, without any inconsistency in the upper bounds of the BR in the LFV decays of charged leptons. In order to find the reasonable regions of parameter space, the upper bounds must be checked in the formula given in [17]:

$$\frac{\sum_{a=1}^3 [(y^\dagger_L)_{af}(y_L)_{ia}]^2 (I_{1,a}I_{2,a} + I^2_{1,a}) + \sum_{a=1}^3 [(y_R)_{af}(y^\dagger_R)_{ia}]^2 (I'_{1,a}I'_{2,a} + I'^2_{1,a})}{16 m^4_{h^\pm_1} |\sum_{a=1}^3 (I_{1,a}I_{2,a} + I^2_{1,a})|} < \frac{C_{if}}{[\text{TeV}]^4}, \quad (20)$$

where $(i, f) = (\mu, e) = (2, 1)$, $C_{if} = 1.6 \times 10^{-6}$, and many notations, including $(I_{1,a}, I_{2,a}, I'_{1,a}, I'_{2,a})$, are defined in detail in [17]. For simplicity, we mention only the following special cases. In the limit $0 \simeq m_{\nu_a} \ll m_{h^\pm_1}$ and $m_{h^\pm_2} \gg m_{N_1}$, we have

$$I_{1,a} \simeq -\frac{1}{(4\pi)^2}\frac{1}{36 m^2_{h^\pm_1}}, \quad I_{2,a} \simeq -\frac{1}{(4\pi)^2}\frac{5}{36 m^2_{h^\pm_1}},$$
$$I'_{1,a} \simeq -\frac{1}{(4\pi)^2}\frac{1}{36 m^2_{h^\pm_2}}, \quad I'_{2,a} \simeq -\frac{1}{(4\pi)^2}\frac{5}{36 m^2_{h^\pm_2}}. \quad (21)$$

While a very large m_{N_a} gives $I'_{1,a}, I'_{2,a} \simeq 0$—for example, when $m_{N_{2,3}}$ are larger than a few TeV—the bound (20) affects only the products $|(y^\dagger_L)_{31}(y_L)_{23}|$ and $|(y_R)_{31}(y_R)^\dagger_{23}|$. Combining this with (18), we get new constraints:

$$|(y_L)_{23}| \leq 0.149 \frac{m_{h^\pm_1}}{1\ \text{TeV}},$$
$$\text{and} \quad |(y_R)_{31}(y^\dagger_R)_{23}| < \left(\frac{0.1 m_{h^\pm_2}}{1\ \text{TeV}}\right)^2. \quad (22)$$

This constraint of $|(y_L)_{23}|$ is consistent with the numerical investigation done in [17], where $m_{h^\pm_1} = 4.8$ TeV prefers $(y_L)_{23} = 0.5$–$0.6 < 0.7 \simeq 4.8 \times 0.15$. Interestingly, the first inequality in (22) is more strict than the one given in (19). The second constraint in (22) suggests that the small $|(y_R)_{31}|$ will allow for a large $|(y^\dagger_R)_{23}|$; i.e., the choice of $|(y_R)_{31}| \leq 10^{-3} \times (m_{h^\pm_2}/1\ \text{TeV})^2$ will allow $|(y^\dagger_R)_{23}| \sim \mathcal{O}(1)$. $m_{h^\pm_2} = 5(3)$ TeV will give $|(y_R)_{31}| \leq 0.25(0.09)$, consistent with the promoting regions indicated in [17]. However, the absolute values of $(y_R)_{22}$ and

$(y_R)_{23}$ should be smaller than the perturbative upper bound 4π.

Another relevant constraint is the small upper bound of $\mathrm{BR}(\mu \to 3e)$. Following [17], all form factors relating to $(y_R)_{ij}$ contain at least three factors, $(y_R)_{i1}$ or $(y_R)_{1i}$. Therefore, they result in very suppressed values of the BR of the LFVHD if all $|(y_R)_{i1,1i}|$'s are small enough, without any conditions of small $|(y_R)_{23,32,33}|$'s.

Combining the above discussion with the analysis in [17], the reasonable values of the free parameters can be chosen as follows: $s_\alpha = 0.3$, $\lambda \equiv 8\lambda_{\Phi h_1} = 8\lambda_{\Phi h_2} = \lambda_{\Sigma h_1} = \lambda_{\Sigma h_2} = 4$, $m_{h_1^\pm} = m_{h_2^\pm} = 3$ TeV, $m_H = 2$ TeV, $(y_L)_{23} = \frac{0.14 m_{h_1^\pm}}{1\ \mathrm{TeV}}$, $y'_R = (y_R)_{23} = (y_R)_{32} = (y_R)_{33} = 3$, $(y_R)_{22} = 8$, $v' \in \{1, 2, 8, 10\}$ TeV, $m_{N_1} = m_h/2$, $m_{N_2} = 1/2 m_{N_3} = 5$ TeV, and $(y_R)_{i,j} = 10^{-2}$, with at least one of the indices, i or j, being 1. We would like to stress that the above choices are also based on the following additional reasons. The values of $(y_L)_{23}$ and $(y_R)_{ij}$ always satisfy all recent bounds of the BR of the LFV decays of charged leptons (22) as well as gauge coupling universalities (19). The λ parameter is positive and small enough to satisfy the conditions of both the perturbative limit and vacuum stability, whereas it is large enough to enhance the BR of the LFVHD.

To investigate the variance of $\mathrm{BR}(h \to \mu\tau)$ versus the changing of free parameters, the ranges of free parameters will be chosen as follows: $|s_\alpha| \le 0.4$, $0.1 < \lambda < 10$, $|y'_R| \le 4$, $|(y_L)_{23}| \le \frac{0.15 m_{h_1^\pm}}{1\ \mathrm{TeV}}$, $1\ \mathrm{TeV} \le m_{h_1^\pm}, m_{h_2^\pm}$, $v' < 10$ TeV and $0.5\ \mathrm{TeV} \le m_{N_2} \le 6$ TeV.

IV. NUMERICAL RESULT AND DISCUSSION

In this section, we will first investigate some private contributions to the BR of the LFVHD, namely, the active neutrino loops with $W^\pm/h_1^\pm$ bosons, and the exotic lepton loops. Based on this, the parameter space regions which give the large total contribution will be further studied.

The contributions of active neutrinos are shown in Fig. 2. The left panel shows two contributions to $\mathrm{Br}(h \to \mu\tau)$: the sum of all diagrams relating to the $W^\pm$ gauge bosons and their Goldstone bosons, and Fig. 1(f). The right panel shows the contribution to $\mathrm{Br}(h \to \mu\tau)$ from Fig. 1(d), with a virtual $h_1^\pm$ in the loop. The figure emphasizes two points: the tiny contributions in the left panel and the significantly enhanced contribution in the right panel. Similarly to many well-known models, the total contribution of electroweak loops, including $W^\pm$ and their Goldstone bosons, is very suppressed because of the GIM mechanism, arising from the sum of two different flavors of external lepton fields: $\sum_a U^L_{2a} U^{L*}_{3a} = 0$. This sum cancels the largest terms of the contributions when they are expanded in terms of the $(m_{\nu_a}/m_W)^2$ series. Only terms containing the factors $(m_{\nu_a}/m_W)^2$ survive, but they are very suppressed. In addition, this contribution does not depend on v', leading to the overlap lines in the left panel of the figure. The second contribution in the left panel comes from the $\nu\nu h_1^\pm$ loops. Although the appearance of the Yukawa couplings $(y_L)_{ij}$ removes the GIM mechanism, the contribution itself contains a factor of $m^2_{\nu_a}$; therefore, it is suppressed, too. It is even smaller than the electroweak-loop contribution because $m_{h_1^\pm}$ is much larger than m_W. $\nu h_1^\pm h_1^\pm$ is much enhanced because of the presence of both the large coupling $\lambda_{h h_1^\pm h_1^\pm}$ and y_L. In the model considered, $|(y_L)_{23}|$ is significantly constrained from (22), where the $m_{h_1^\pm} = 3$ TeV gives the small $|(y_L)_{23}| < 0.45$. Also, $\lambda_{h h_1^\pm h_1^\pm}$, as a function of $v'(<10\ \mathrm{TeV})$ and Higgs self-couplings $(<4\pi)$, does not allow large values of $\mathrm{Br}(h \to \mu\tau)$. Then the contribution of the $\nu\nu h_1^\pm$ loop to the $\mathrm{Br}(h \to \mu\tau)$ is not larger than 10^{-10}. In any case, this provides a hint for enhancing the contribution from active neutrino loops, for example, in models with a four-loop (or

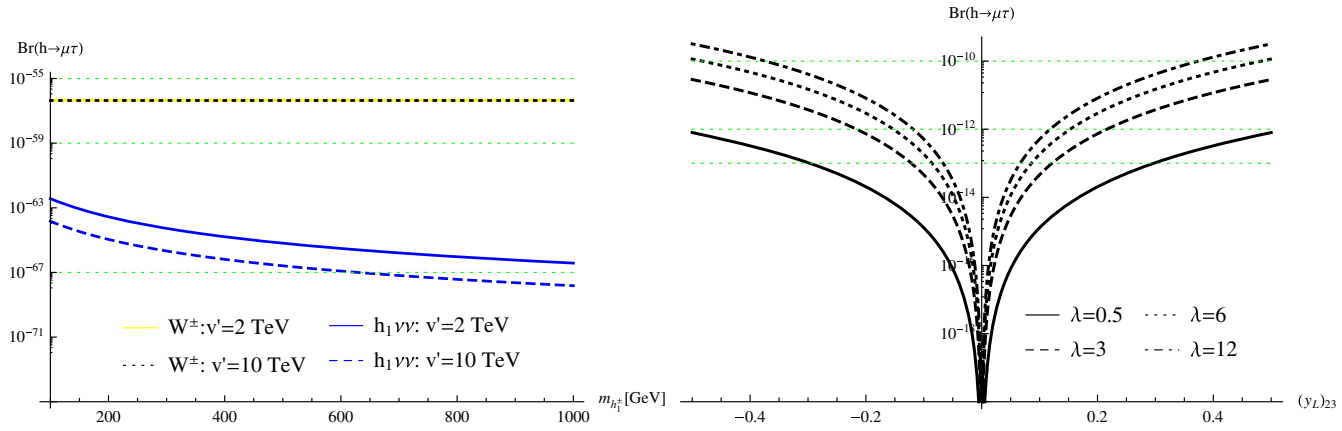

FIG. 2. Private contributions of active neutrino loops only to the $\mathrm{Br}(h \to \mu\tau)$, where on the left-hand side it is assumed that $(y_L)_{23} = \frac{0.14 m_{h_1^\pm}}{1\ \mathrm{TeV}}$ and the right-hand side corresponds to $v' = 10$ TeV.

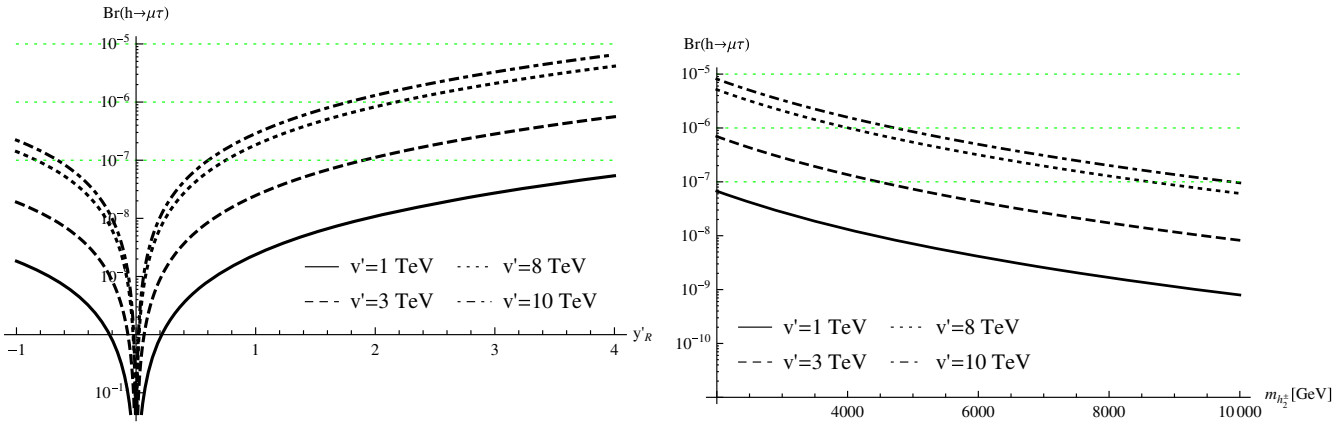

FIG. 3. Private contributions of $Nh_2^{\pm}h_2^{\pm}$ loops only, i.e., Fig. 1(d), to $\mathrm{Br}(h \to \mu\tau)$ as a function of y'_R (m_{h_2}) in the left (right) panel.

higher) neutrino mass and a small $m_{h_1^{\pm}}$, where the constraint of y_L may be released. This deserves further study.

The main contributions of exotic leptons to $\mathrm{Br}(h \to \mu\tau)$ come from the two diagrams $Nh_2^{\pm}h_2^{\pm}$ and $h_2^{\pm}NN$. They do not depend on y_L but depend strongly on $|(y_R)_{ij}|$, with $\{i, j\} = \{2, 3\}$. As illustrated in Figs. 3 and 4, the two contributions have common properties. They increase with a decreasing $m_{h_2^{\pm}}$, in the same behavior shown in the right panel of Fig. 3. Most important is that they are enhanced strongly with an increasing $|y'_R|$; see the two left panels in the two figures.

On the other hand, these two contributions behave in opposing ways with the changes of v' and $m_{N_2}(m_{N_3})$. The contribution from the m_{N_1} mediation is ignored because of a very small $|(y_R)_{i1,1i}|$ ($i = 1, 2, 3$). The $Nh_2^{\pm}h_2^{\pm}$ mediation relates with the Higgs self-coupling; hence, its contribution is large with a small m_{N_2} and a large v'. See Fig. 3 with its four fixed values of v', where the largest corresponds to $v' = 10$ TeV. For the $h_2^{\pm}NN$ loops, their analytic expression contains $m_{N_a}^2/v'$ factors separate from the C functions. Therefore, the small v' and large m_{N_a} will give large contributions; see the right panel of Fig. 4.

All of the above discussions suggest that $\mathrm{Br}(h \to \mu\tau)$ will be large with small singly charged Higgs masses and large values of all of the following parameters: the coupling $|y'_R|$, $|(y_L)_{23}|$, and the Higgs self-coupling λ. The dependence of the BR on v' and $m_{N_{2,3}}$ is a bit complicated. The dependence on the mixing angle α of two CP-even neutral Higgs bosons should also be mentioned. Figure 5 shows more precisely the variations of $\mathrm{Br}(h \to \mu\tau)$ on some particular free parameters. We can realize that y'_R affects the change of this BR most significantly. It is larger than 10^{-6} only when $|y'_R| \geq 2$. $\mathrm{Br}(h \to \mu\tau)$ does not depend on the signs of s_α and y'_R, but it does depend significantly on the absolute values of these parameters. With $\lambda = 4$, $m_{h_2^{\pm}} = 3$ TeV, and $s_\alpha = 0.3$, the $\mathrm{Br}(h \to \mu\tau)$ can reach 10^{-5} when all of these conditions are satisfied: $|y'_R| \geq 3$, $v' \geq 8$ TeV, and $m_{N_{2,3}}$ are small enough.

Finally, if the doubly charged Higgs bosons are heavy enough, the investigation shown in [17] may allow the presence of a light, singly charged Higgs boson $h_2^{\pm}$, for instance, with the mass of 1 TeV. Besides, if we define $m_{N_2} = m_{N_3}/2 = f \times v'$, adopting also that $s_\alpha = 0.3$ gives $v' \leq 9$ TeV [17,23]. In addition, if $y'_R = 4$, then BR$(h \to \mu\tau)$

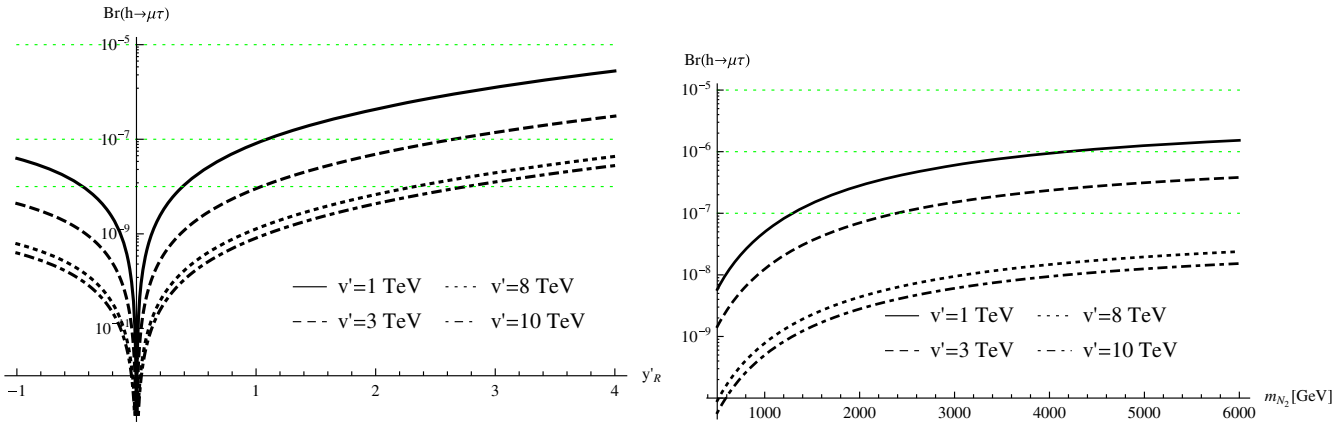

FIG. 4. Private contributions of the $h_2^{\pm}NN$ loops only, i.e., Fig. 1(f), to the $\mathrm{Br}(h \to \mu\tau)$ as a function of y'_R (m_{N_2}) in the left (right) panel.

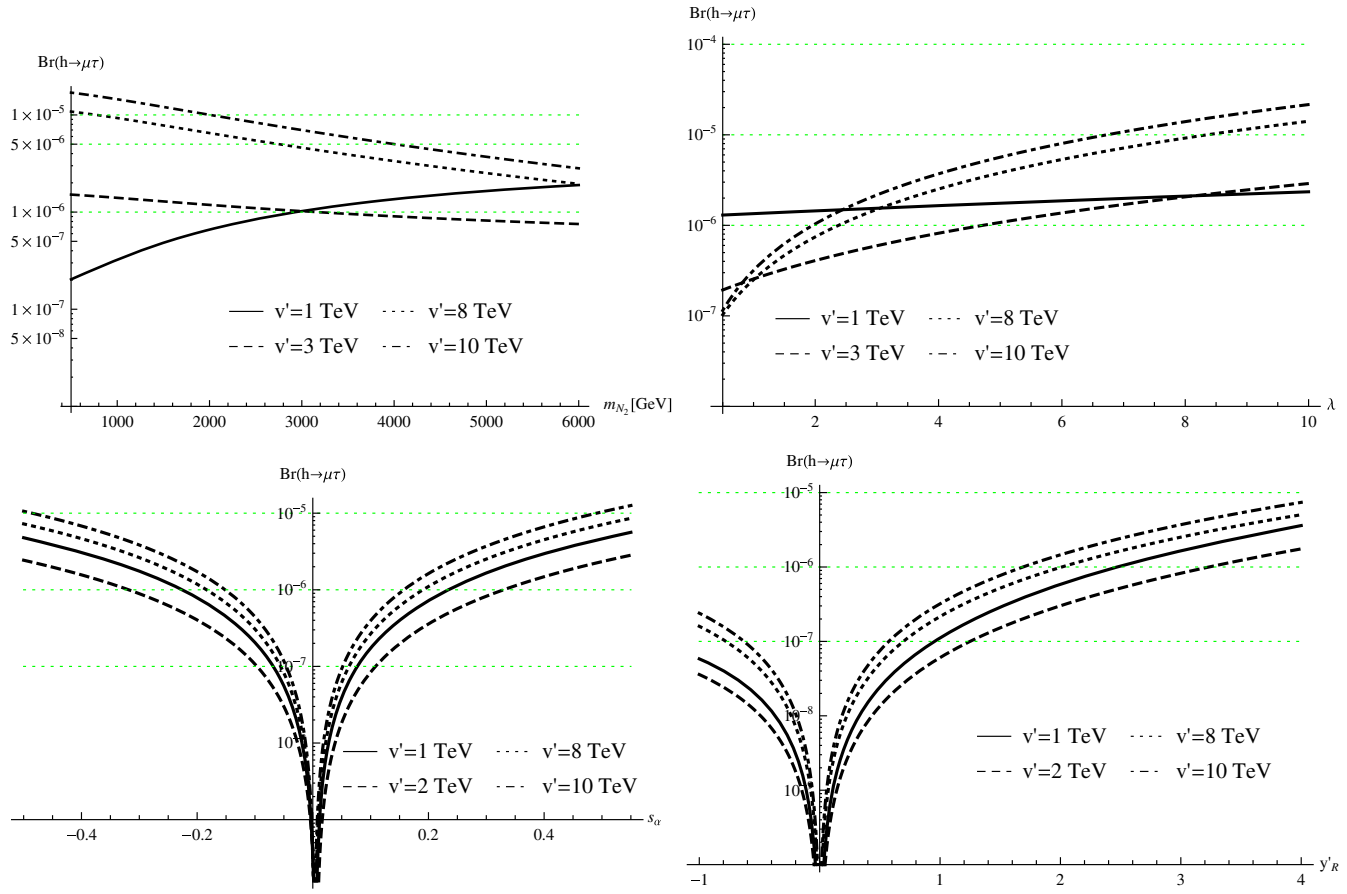

FIG. 5. The total contribution to $\mathrm{Br}(h \to \mu\tau)$ as a function of the single parameters m_{N_2}, λ, s_α, and y'_R.

can reach the value of 10^{-4}, very close to the value noted by CMS. This conclusion is illustrated in Fig. 6, where the f parameter is scanned in the range of $0.1 \leq f \leq 6$ ($0.1 \leq f \leq 2$) in the left (right) panel. From our numerical calculation, the values of $y'_R = 4$ and $m_{h_1^\pm} = 1$ TeV are the smallest ones to obtain values about 10^{-4} of $\mathrm{Br}(h \to \mu\tau)$. Accordingly, this large value lies in the only region where v' is larger than 4 TeV, while m_{N_2} and m_{N_3} should be as small as possible. In this calculation, $m_{N_2} \geq 400$ GeV and the $Nh_2^\pm h_2^\pm$ contribution is dominant. With a small $v' \simeq 1$ TeV, the value around 10^{-5} of $\mathrm{Br}(h \to \mu\tau)$ may occur if $m_{N_{2,3}}$ are large enough: $m_{N_2} \geq 3v'$. Also, $\mathrm{Br}(h \to \mu\tau)$ is unchanged, with

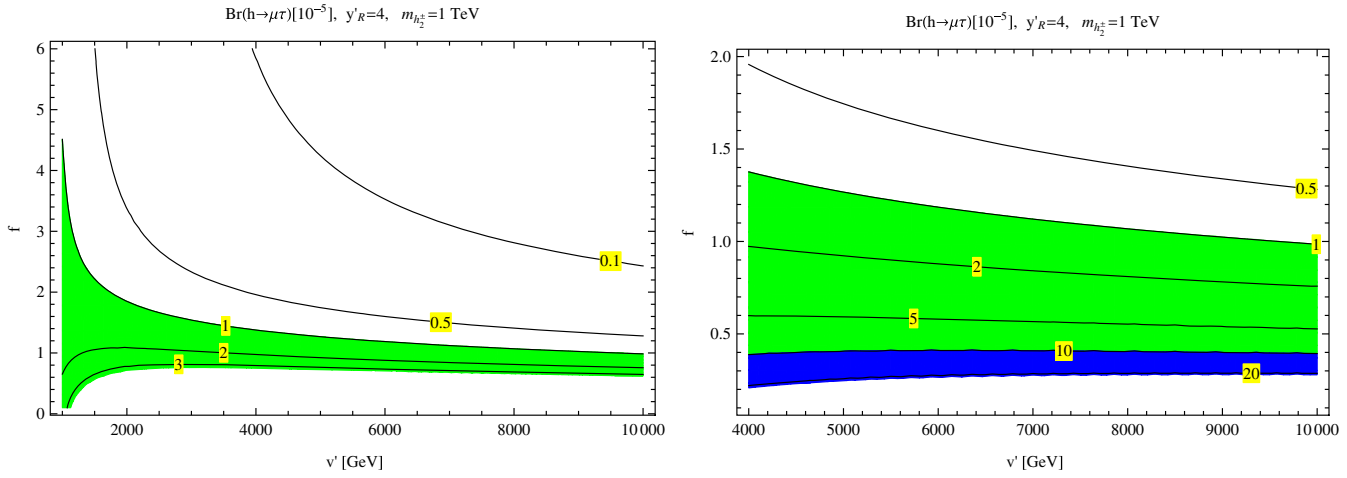

FIG. 6. Contour plots of $\mathrm{Br}(h \to \mu\tau)$ as functions of v' and $f = m_{N_2}/v'$. The green and blue regions satisfy $10^{-5} \leq \mathrm{BR}(h \to \mu\tau) \leq 10^{-4}$ and $\mathrm{BR}(h \to \mu\tau) \geq 10^{-4}$, respectively.

the general condition $m_{N_2} \leq m_{N_3}$, instead of the $M_{N_2} = 1/2M_{N_3}$ one used above. In this case, the large LFVHD corresponds to the dominant contribution from the $h_2^\pm NN$ diagram. The heavy neutrinos may be detected in future lepton colliders [24].

The singly charged Higgs bosons are now being researched by experiments [21,25]. However, in the model considered, none of them are their targets because they only couple with leptons. In addition, the $h_2^\pm$'s hold negative parities and hence cannot decay to only normal leptons. We also believe that the condition (22) is enough to guarantee constraints of LFV processes without the need for singly charged Higgs bosons that are too heavy. Hence, the mass around 1 TeV of $h_2^\pm$ is reasonable for stability of the lightest N_{R_1} as a dark matter candidate.

V. CONCLUSION

Radiative neutrino mass models are interesting ones for explaining the tiny masses of active neutrinos. In the model introduced in [17], the new parameters that generate neutrino masses radiatively are strongly constrained from recent experimental data such as neutrino oscillations, the rare decay of charged leptons, gauge coupling universalities, and other constraints from LHC Higgs boson physics. Therefore, these parameters are very predictive for other phenomenologies such as dark matter, the LFVHD, etc. In this work, we have shown that, in the allowed region with heavy, singly charged Higgs bosons, where their masses are around 3 TeV, the BR of the LFVHD can reach a value of 10^{-5}. If the mass of the $h_2^\pm$ is around 1 TeV, the $\mathrm{Br}(h \to \mu\tau)$ can reach 10^{-4}. The additional necessary conditions are that v', $|s_\alpha|$, and all amplitudes of the Yukawa and trilinear Higgs couplings must be large enough. For example, with the largest $s_\alpha = 0.3$ to satisfy the LHC Higgs boson constraint, v' should be in the range of 8 to 9 TeV. Also, $\lambda_{\Sigma h_2} \geq 4$ and $|y'_R| \geq 3$ (4) for the largest values 10^{-5} (10^{-4}) of the $\mathrm{Br}(h \to \mu\tau)$. The masses of the two heavy exotic neutrinos should be small, around 400 GeV for the lighter m_{N_2}. In the model under consideration, a large $\mathrm{BR}(h \to \mu\tau)$ will lead to necessary consequences: the doubly charged Higgs bosons $k^{\pm\pm}$ must be heavy and $\mathrm{BR}(h \to e\tau)$ must be very small. The latter can be explained from the constraint of $\mu \to e\gamma$. This requires a large $y'_R \simeq \mathcal{O}(1)$ to give a very small $|(y_R)_{13,31}| \leq 10^{-3}$, implying that $\mathrm{BR}(h \to e\tau) \leq 10^{-10}$, much smaller than the recent sensitivity of experiments [4]. One more interesting property is that the contribution of the virtual active neutrinos may be large if the upper bound (22) is ignored. When this bound is considered, the private contributions of $\nu h_1^\pm h_1^\pm$ to $\mathrm{Br}(h \to \mu\tau)$ are around 10^{-10}, which is much larger than the values predicted by canonical seesaw models and [10]. In models with more than three-loop neutrino mass such as [26], the bound (22) may be released. We then guess that the active neutrino contributions can reach 10^{-7} or higher, and hence they should not be ignored. In conclusion, more precise predictions will be possible after we receive updated data from experiments in the near future.

ACKNOWLEDGMENTS

The authors thank Dr. Farinaldo Queiroz for his comments on DM. This research is funded by the Vietnam National Foundation for Science and Technology Development (NAFOSTED) under Grant No. 103.01-2015.33.

APPENDIX A: ONE-LOOP PASSARINO-VELTMAN FUNCTIONS

The calculation in this section relates to the one-loop diagrams in Fig. 1. The analytic expressions of the PV function are given in [10], and the needed formulas will be summarized in this appendix. We would like to stress that these PV functions were derived from the general form given in [27], using only the conditions of very small masses of tauons and muons. They are consistent with [28]. The denominators of the propagators are denoted as $D_0 = k^2 - M_0^2 + i\delta$, $D_1 = (k - p_1)^2 - M_1^2 + i\delta$, and $D_2 = (k + p_2)^2 - M_2^2 + i\delta$, where δ is an infinitesimally positive real quantity. The scalar integrals are defined as

$$\begin{aligned} B_0^{(1)} &\equiv \frac{(2\pi\mu)^{4-D}}{i\pi^2}\int \frac{d^Dk}{D_0D_1}, \\ B_0^{(2)} &\equiv \frac{(2\pi\mu)^{4-D}}{i\pi^2}\int \frac{d^Dk}{D_0D_2}, \\ B_0^{(12)} &\equiv \frac{(2\pi\mu)^{4-D}}{i\pi^2}\int \frac{d^Dk}{D_1D_2}, \\ C_0 &\equiv C_0(M_0,M_1,M_2) = \frac{1}{i\pi^2}\int \frac{d^4k}{D_0D_1D_2}, \end{aligned} \tag{A1}$$

where $i = 1, 2$. In addition, $D = 4 - 2\epsilon \leq 4$ is the dimension of the integral; M_0, M_1, M_2 are masses of virtual particles in the loop. The momenta satisfy the conditions $p_1^2 = m_1^2$, $p_2^2 = m_2^2$, and $(p_1 + p_2)^2 = m_h^2$. In this work, m_1 and m_2 are the respective masses of the muon and the tauon, and m_h is the SM-like Higgs boson mass. The tensor integrals are

$$\begin{aligned} B^\mu(p_i;M_0,M_i) &= \frac{(2\pi\mu)^{4-D}}{i\pi^2}\int \frac{d^Dk\times k^\mu}{D_0D_i} \equiv B_1^{(i)}p_i^\mu, \\ B^\mu(p_1,p_2;M_1,M_i) &= \frac{(2\pi\mu)^{4-D}}{i\pi^2}\int \frac{d^Dk\times k^\mu}{D_1D_2} \\ &\equiv B_1^{(12)}p_1^\mu + B_2^{(12)}p_2^\mu, \\ C^\mu &= C^\mu(M_0,M_1,M_2) \\ &= \frac{1}{i\pi^2}\int \frac{d^4k\times k^\mu}{D_0D_1D_2} \equiv C_1p_1^\mu + C_2p_2^\mu, \end{aligned} \tag{A2}$$

where $B_{0,1}^{(i)}$ and $C_{0,1,2}$ are PV functions. It is well known that C_i is finite, while the remains are divergent. We define $\Delta_\epsilon \equiv \frac{1}{\epsilon} + \ln 4\pi - \gamma_E + \ln\frac{\mu^2}{m_h^2}$, where γ_E is the Euler constant. The divergent parts of the above scalar factors can be determined as

$$\begin{aligned} \mathrm{Div}[B_0^{(i)}] &= \mathrm{Div}[B_0^{(12)}] = \Delta_\epsilon, \\ \mathrm{Div}[B_1^{(1)}] &= -\mathrm{Div}[B_1^{(2)}] = \frac{1}{2}\Delta_\epsilon. \end{aligned} \tag{A3}$$

The finite parts of the PV functions such as B functions depend on the scale of a μ parameter with the same coefficient of the divergent parts.

The analytic formulas of the above PV functions are

$$B_{0,1}^{(i)} = \mathrm{Div}[B_{0,1}^{(i)}] + b_{0,1}^{(i)}, \qquad B_{0,1,2}^{(12)} = \mathrm{Div}[B_{0,1,2}^{(12)}] + b_{0,1,2}^{(12)}. \tag{A4}$$

The expression of $b_0^{(12)}$ is

$$b_0^{(12)} = \ln\frac{m_h^2 - i\delta}{M_1^2 - i\delta} + 2 + \sum_{k=1}^{2} x_k \ln\left(1 - \frac{1}{x_k}\right), \tag{A5}$$

where x_k, $(k = 1, 2)$ are solutions of the equation

$$x^2 - \left(\frac{m_h^2 - M_1^2 + M_2^2}{m_h^2}\right)x + \frac{M_2^2 - i\delta}{m_h^2} = 0. \tag{A6}$$

The C_0 function was given in [10], consistent with that discussed in [28], namely,

$$C_0 = \frac{1}{m_h^2}[R_0(x_0, x_1) + R_0(x_0, x_2) - R_0(x_0, x_3)], \tag{A7}$$

where

$$R_0(x_0, x_i) \equiv Li_2\left(\frac{x_0}{x_0 - x_i}\right) - Li_2\left(\frac{x_0 - 1}{x_0 - x_i}\right), \tag{A8}$$

$Li_2(z)$ is the dilogarithm function, $x_{1,2}$ are solutions of Eq. (A6), and $x_{0,3}$ are given as

$$x_0 = \frac{M_2^2 - M_0^2}{m_h^2}, \qquad x_3 = \frac{-M_0^2 + i\delta}{M_1^2 - M_0^2}. \tag{A9}$$

For simplicity of calculation, we use approximate forms of PV functions where $p_1^2,\ p_2^2 \to 0$, namely,

$$\begin{aligned} b_0^{(i)} &= 1 - \ln\frac{M_i^2}{m_h^2} + \frac{M_0^2}{M_0^2 - M_i^2}\ln\frac{M_i^2}{M_0^2}, \\ b_1^{(1)} &= -\frac{1}{2}\ln\frac{M_1^2}{m_h^2} - \frac{M_0^4}{2(M_0^2 - M_1^2)^2}\ln\frac{M_0^2}{M_1^2} \\ &\quad + \frac{(M_0^2 - M_1^2)(3M_0^2 - M_1^2)}{4(M_0^2 - M_1^2)^2}, \\ b_1^{(2)} &= \frac{1}{2}\ln\frac{M_2^2}{m_h^2} + \frac{M_0^4}{2(M_0^2 - M_2^2)^2}\ln\frac{M_0^2}{M_2^2} \\ &\quad - \frac{(M_0^2 - M_2^2)(3M_0^2 - M_2^2)}{4(M_0^2 - M_2^2)^2}, \\ b_0^{(12)} &= \ln\frac{m_h^2 - i\delta}{M_1^2 - i\delta} + 2 + \sum_{k=1}^{2} x_k \ln\left(1 - \frac{1}{x_k}\right), \\ C_1 &= \frac{1}{m_h^2}[b_0^{(1)} - b_0^{(12)} + (M_2^2 - M_0^2)C_0], \\ C_2 &= -\frac{1}{m_h^2}[b_0^{(2)} - b_0^{(12)} + (M_1^2 - M_0^2)C_0]. \end{aligned}$$

If $M_1 = M_2$, it can be seen that $b_1^{(1)} = -b_1^{(2)}$, $b_0^{(1)} = b_0^{(1)}$, and $C_1 = -C_2$.

APPENDIX B: FORM FACTORS FOR THE LFVHD IN 't HOOFT–FEYNMAN GAUGE

In this section we will list all of the factors for calculating the LFVHD in the model considered. The calculation is done in the 't Hooft–Feynman gauge. The Feynman rules are given in Fig. 7. These factors were cross-checked using FORM [29].

Contribution from Fig. 1(a):

$$i\mathcal{M}_{(1a)} = \frac{ig^2 G_{hWW}}{16\pi^2}\sum_{a=1}^{3} U_{2a}^L U_{3a}^{L*} \times ([\overline{u_1}P_L v_2] \times E_L^{\nu WW} + [\overline{u_1}P_R v_2] \times E_R^{\nu WW}), \tag{B1}$$

where $E_L^{\nu WW} = m_1 m_W C_1$, $E_R^{\nu WW} = -m_2 m_W C_2$, and $C_i \equiv C_i(m_{\nu_a}, m_W, m_W)$.

Contribution from Fig. 1(b):

$$i\mathcal{M}_{(b)} = \frac{igG_{hWG_w}}{16\pi^2}\sum_{a=1}^{3} U_{2a}^L U_{3a}^{L*} \times ([\overline{u_1}P_L v_2]E_L^{\nu WG_w} + [\overline{u_1}P_R v_2]E_R^{\nu WG_w}), \tag{B2}$$

where

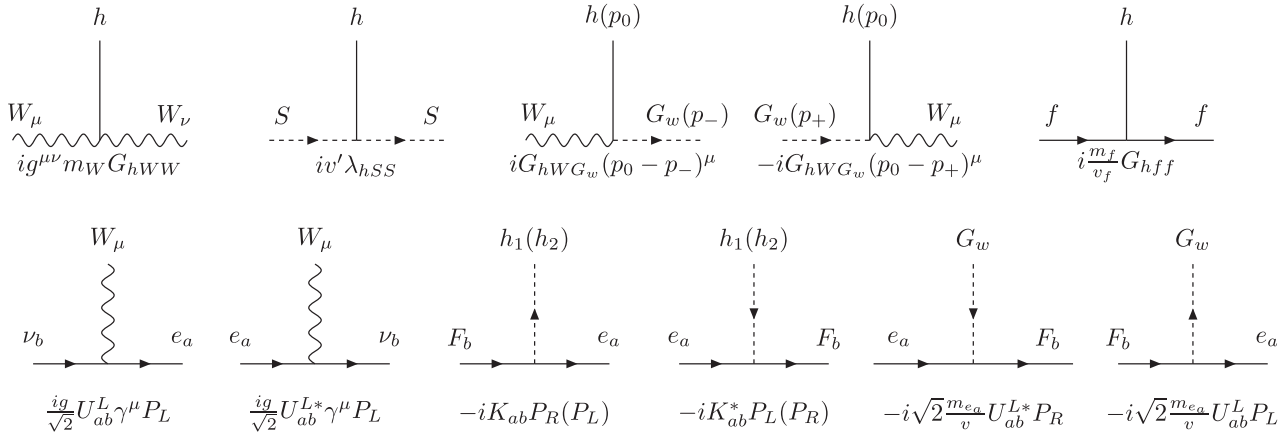

FIG. 7. Feynman rules for $h \to \mu^\pm\tau^\mp$ in the 't Hooft–Feynman gauge. Notations are (i) $S = G_w, h_1^\pm, h_2^\pm$; (ii) $K_{ab} = (y_L^T U^L)_{ab}$ and $(y_R^T)_{ab}$, for active and exotic neutrinos, respectively; and (iii) $f = e_a, \nu_a, N_a$, $F_a = \nu_a, N_a$.

$$E_L^{\nu WG_w} = -\frac{m_1 m_2^2}{v}(2C_1 - C_2),$$
$$E_R^{\nu WG_w} = -\frac{m_2}{v}(B_0^{(12)} + m_{\nu_a}^2 C_0 - m_1^2 C_1 + 2m_2^2(-C_1 + C_2) + 2m_h^2 C_1), \tag{B3}$$

and $B_0^{(12)} \equiv B_0^{(12)}(m_W, m_W)$, $C_i \equiv C_i(m_{\nu_a}, m_W, m_W)$.

Contribution from Fig. 1(c):

$$i\mathcal{M}_{(c)} = \frac{igG_{hWG_w}}{16\pi^2}\sum_{a=1}^{3} U^L_{2a}U^{L*}_{3a} \times ([\overline{u_1}P_L v_2]E_L^{\nu G_w W} + [\overline{u_1}P_R v_2]E_R^{\nu G_w W}), \tag{B4}$$

where

$$E_L^{\nu G_w W} = -\frac{m_1}{v}(B_0^{(12)} + m_{\nu_a}^2 C_0 + 2m_1^2(-C_1 + C_2) + m_2^2 C_2 - 2m_h^2 C_2),$$
$$E_R^{\nu G_w W} = -\frac{m_1^2 m_2}{v}(C_1 - 2C_2), \tag{B5}$$

and $B_0^{(12)} \equiv B_0^{(12)}(m_W, m_W)$, $C_i \equiv C_i(m_{\nu_a}, m_W, m_W)$.

Contribution from Fig. 1(d):

$$i\mathcal{M}_{(d)} = \frac{i(v'\lambda_{hSS})}{16\pi^2}\sum_{a=1}^{3} V_{2a}V^*_{3a} \times ([\overline{u_1}P_L v_2]E_L^{FSS} + [\overline{u_1}P_R v_2]E_R^{FSS}), \tag{B6}$$

where $C_i \equiv C_i(m_a, m_S, m_S)$, $V = \{U^L, K, y_R^T\}$, $m_a = \{m_{\nu_a}, m_{N_a}\}$ for $S = \{G_w, h_1, h_2\}$, and

$$E_L^{\nu G_w G_w} = \frac{m_1 m_2^2}{v^2}2C_2, \qquad E_R^{\nu G_w G_w} = \frac{m_1^2 m_2}{v^2}(-2C_1), \qquad E_L^{\nu h_1 h_1} = -m_1 C_1,$$
$$E_R^{\nu h_1 h_1} = m_2 C_2; \qquad E_L^{N h_2 h_2} = m_2 C_2, \qquad E_R^{N h_2 h_2} = -m_1 C_1, \tag{B7}$$

Contribution from Fig. 1(e):

$$i\mathcal{M}_{(e)} = \frac{ig^2 G_{h\nu\nu}}{16\pi^2}\sum_{a=1}^{3} U^L_{2a}U^{L*}_{3a}([\overline{u_1}P_L v_2]E_L^{W\nu\nu} + [\overline{u_1}P_R v_2]E_R^{W\nu\nu}), \tag{B8}$$

where

$$E_L^{W\nu\nu} = -\frac{m_1 m_{\nu_a}^2}{v'}(C_0 - 2C_1), \qquad E_R^{W\nu\nu} = -\frac{m_2 m_{\nu_a}^2}{v'}(C_0 + 2C_2), \tag{B9}$$

and $C_i \equiv C_i(m_W, m_{\nu_a}, m_{\nu_a})$.

Contribution from Fig. 1(f):

$$i\mathcal{M}_{(f)} = \frac{iG_{hFF}}{16\pi^2}\sum_{a=1}^{3} V_{2a}V_{3a}^*([\overline{u_1}P_L v_2]E_L^{SFF} + [\overline{u_1}P_R v_2]E_R^{SFF}), \tag{B10}$$

where $C_i \equiv C_i(m_S, m_a, m_a)$, $V = \{U^L, K\}$, $m_a = \{m_{\nu_a}, m_{N_a}\}$ for $S = \{G_w, h_1, h_2\}$, and

$$E_L^{G_w\nu\nu} = -\frac{m_1 m_{\nu_a}^2}{v'}\left[\frac{m_2^2}{v^2}2(C_0 + 2C_2)\right], \qquad E_R^{G_w\nu\nu} = -\frac{m_2 m_{\nu_a}^2}{v'}\left[\frac{m_1^2}{v^2}2(C_0 - 2C_1)\right], \qquad E_L^{h_1\nu\nu} = -\frac{m_1 m_{\nu_a}^2}{v'}(C_0 - 2C_1),$$
$$E_R^{h_1\nu\nu} = -\frac{m_2 m_{\nu_a}^2}{v'}(C_0 + 2C_2), \qquad E_L^{h_2NN} = -\frac{m_2 m_{N_a}^2}{v'}(C_0 + 2C_2), \qquad E_R^{h_2NN} = -\frac{m_1 m_{N_a}^2}{v'}(C_0 - 2C_1), \tag{B11}$$

Contribution from the sum of Figs. 1(g) and 1(h):

$$i\mathcal{M}_{(gh)} = \frac{ig^2 G_{hee}}{16\pi^2}\sum_{a=1}^{3} U_{2a}^L U_{3a}^{L*}([\overline{u_1}P_L v_2]E_L^{\nu W} + [\overline{u_1}P_R v_2]E_R^{\nu W}), \tag{B12}$$

where

$$E_L^{\nu W}(m_F, m_W) = -\frac{m_1 m_2^2}{(m_1^2 - m_2^2)v}[B_1^{(1)} + B_1^{(2)}], \qquad E_R^{\nu W}(m_F, m_W) = \frac{m_1}{m_2}E_L^{\nu W}, \tag{B13}$$

$B_1^{(i)} \equiv B_1^{(i)}(m_{\nu_a}, m_W)$.

Contribution from the sum of Figs. 1(i) and 1(j):

$$i\mathcal{M}_{(ik)} = \frac{iG_{hee}}{16\pi^2}\sum_{a=1}^{3} V_{2a}V_{3a}^*([\overline{u_1}P_L v_2]E_L^{FS} + [\overline{u_1}P_R v_2]E_R^{FS}), \tag{B14}$$

where $B_1^{(i)} \equiv B_1^{(i)}(m_a, m_S)$, $V = \{U^L, K, y_R^T\}$, $m_a = \{m_{\nu_a}, m_{N_a}\}$ for $S = \{G_w, h_1, h_2\}$, and

$$E_L^{\nu G_w} = -\frac{2m_1^3 m_2^2}{(m_1^2 - m_2^2)v^3}(B_1^{(1)} + B_1^{(2)}), \qquad E_R^{\nu G_w} = \frac{m_2}{m_1}E_L^{\nu G_w}, \qquad E_L^{\nu h_1} = \frac{-m_1 m_2^2}{(m_1^2 - m_2^2)v}(B_1^{(1)} + B_1^{(2)}),$$
$$E_R^{\nu h_1} = \frac{m_1}{m_2}E_L^{\nu h_1}, \qquad E_L^{Nh_2} = -\frac{m_1^2 m_2}{(m_1^2 - m_2^2)v}(B_1^{(1)} + B_1^{(2)}), \qquad E_R^{Nh_2} = \frac{m_2}{m_1}E_L^{Nh_2}. \tag{B15}$$

The divergence cancellation of the total amplitudes of the LFV decays is proved as follows. The divergences appear only in the expressions listed in (B3), (B5), (B13), and (B15). The expressions in (B3) and (B5) will vanish after inserting them into (B2) and (B4), where the GIM mechanism works. The divergences in each contribution given in (B13) and (B15) cancel each other because $\mathrm{Div}[B_1^{(1)}] = -\mathrm{Div}[B_1^{(2)}]$. Furthermore, the limit $p_1^2, p_2^2 \to 0$ results in $B_1^{(1)} = -B_1^{(2)}$; therefore, all of the aforementioned contributions are very suppressed.

[1] G. Aad *et al.* (ATLAS Collaboration), Phys. Lett. B **716**, 1 (2012).

[2] G. Aad *et al.* (CMS Collaboration), Phys. Lett. B **716**, 30 (2012).

[3] V. Khachatryan *et al.* (CMS Collaboration), Phys. Lett. B **749**, 337 (2015); G. Aad *et al.* (ATLAS Collaboration), J. High Energy Phys. 11 (2015) 211.

[4] CMS Collaboration, Report No. CMS-PAS-HIG-14-040, 2015.

[5] A. Pilaftsis, Phys. Lett. B **285**, 68 (1992); J. G. Körner, A. Pilaftsis, and K. Schilcher, Phys. Rev. D **47**, 1080 (1993); E. Arganda, A. M. Curiel, M. J. Herrero, and D. Temes, Phys. Rev. D **71**, 035011 (2005).

[6] E. Arganda, M. J. Herrero, X. Marcano, and C. Weiland, Phys. Rev. D **91**, 015001 (2015).

[7] A. Brignole and A. Rossi, Phys. Lett. **566**, 217 (2003); Nucl. Phys. **B701**, 3 (2004); M. Arana-Catania, E. Arganda, and M. J. Herrero, J. High Energy Phys. 09 (2013) 160; 10 (2015) 192; E. Arganda, M. J. Herrero, X. Marcano, and C. Weiland, Phys. Rev. D **93**, 055010 (2016); P. T. Giang, L. T. Hue, D. T. Huong, and H. N. Long, Nucl. Phys. **B864**, 85 (2012); L. T. Hue, D. T. Huong, H. N. Long, H. T. Hung, and N. H. Thao, Prog. Theor. Exp. Phys. (**2015**), 113B05; D. T. Binh, L. T. Hue, D. T. Huong, and H. N. Long, Eur. Phys. J. C **74**, 2851 (2014); E. Arganda, M. J. Herrero, R. Morales, and A. Szynkman, J. High Energy Phys. 03 (2016) 055; J. L. Diaz-Cruz, J. High Energy Phys. 05 (2003) 036.

[8] A. Crivellin, G. D'Ambrosio, and J. Heeck, Phys. Rev. Lett. **114**, 151801 (2015); N. Bizot, S. Davidson, M. Frigerio, and J. L. Kneur, J. High Energy Phys. 03 (2016) 073.

[9] N. Bizot, S. Davidson, M. Frigerio, and J. L. Kneur, J. High Energy Phys. 03 (2016) 073; F. J. Botella, G. C. Branco, M. Nebot, and M. N. Rebelo, Eur. Phys. J. C **76**, 161 (2016); S. Kanemura, T. Ota, T. Shindou, and K. Tsumura, Phys. Rev. D **73**, 016006 (2006); M. Arroyo, J. L. Diaz-Cruz, E. Diaz, and J. A. Orduz-Ducuara, arXiv:1306.2343; D. Das and A. Kundu, Phys. Rev. D **92**, 015009 (2015); X. F Han, L. Wang, and J. M. Yang, Phys. Lett. B **757**, 537 (2016).

[10] L. T. Hue, H. N. Long, T. T. Thuc, and T. Phong Nguyen, Nucl. Phys. **B907**, 37 (2016).

[11] S. Baek and Z.-F. Kang, J. High Energy Phys. 03 (2016) 106; S. Baek and K. Nishiwaki, Phys. Rev. D **93**, 015002 (2016).

[12] K. Cheung, W. Y. Keung, and P. Y. Tseng, Phys. Rev. D **93**, 015010 (2016).

[13] W. Altmannshofer, S. Gori, A. L. Kagan, L. Silvestrini, and J. Zupan, Phys. Rev. D **93**, 031301 (2016); X. G. He, J. Tandean, and Y. J. Zheng, J. High Energy Phys. 09 (2015) 093; I. Doršner, S. Fajfer, A. Greljo, J. F. Kamenik, N. Košnik, and Ivan Nišandžic, J. High Energy Phys. 06 (2015) 108; R. Harnik, J. Kopp, and J. Zupan, J. High Energy Phys. 03 (2013) 026; A. Celis, V. Cirigliano, and E. Passemar, Phys. Rev. D **89**, 013008 (2014); A. Dery, A. Efrati, Y. Nir, Y. Soreq, and V. Susi, Phys. Rev. D **90**, 115022 (2014); J. Heeck, M. Holthausen, W. Rodejohann, and Y. Shimizu, Nucl. Phys. **B896**, 281 (2015); A. Crivellin, G. D' Ambrosio, and J. Heeck, Phys. Rev. D **91**, 075006 (2015); J. L. Diaz-Cruz and J. J. Toscano, Phys. Rev. D **62**, 116005 (2000); A. Pilaftsis, Z. Phys. C **55**, 275 (1992); L. D. Lima, C. S. Machado, R. D. Matheus, and L. A. F. D. Prado, J. High Energy Phys. 11 (2015) 074; I. d. M. Varzielas, O. Fischer, and V. Maurer, J. High Energy Phys. 08 (2015) 080; C. F. Chang, C. H. V. Chang, C. S. Nugroho, and T. C. Yuan, arXiv:1602.00680; C.-H. Chen and T. Nomura, arXiv:1602.07519; K. Huitu, V. Keus, N. Koivunen, and O. Lebedev, J. High Energy Phys. 05 (2016) 026.

[14] M. Sher and K. Thrasher, Phys. Rev. D **93**, 055021 (2016).

[15] S. Kanemura, K. Matsuda, T. Ota, T. Shindou, E. Takasugi, and K. Tsumura, Phys. Lett. B **599**, 83 (2004); G. Blankenburg, J. Ellis, and G. Isidori, Phys. Lett. B **712**, 386 (2012); S. Davidson and P. Verdier, Phys. Rev. D **86**, 111701 (2012); S. Bressler, A. Dery, and A. Efrati, Phys. Rev. D **90**, 015025 (2014); D. Aristizabal Sierra and A. Vicente, Phys. Rev. D **90**, 115004 (2014); C. X. Yue, C. Pang, and Y. C. Guo, J. Phys. G **42**, 075003 (2015); S. Banerjee, B. Bhattacherjee, M. Mitra, and M. Spannowsky, arXiv:1603.05952; I. Chakraborty, A. Datta, and A. Kundu, arXiv:1603.06681.

[16] Y. Fukuda *et al.*, Phys. Rev. Lett. **81**, 1562 (1998); **85**, 3999 (2000).

[17] K. Nishiwaki, H. Okada, and Y. Orikasa, Phys. Rev. D **92**, 093013 (2015).

[18] H. K. Dreiner, H. E. Haber, and S. P. Martin, Phys. Rep. **494**, 1 (2010).

[19] M. C. Gonzalez-Garcia, M. Maltoni, and T. Schwetz, J. High Energy Phys. 11 (2014) 052.

[20] Y. Mambrini, S. Profumo, and F. S. Queiroz, arXiv: 1508.06635.

[21] K. A. Olive *et al.* (Particle Data Group Collaboration), Chin. Phys. C **38**, 090001 (2014).

[22] J. Herrero-Garcia, M. Nebot, N. Rius, and A. Santamaria, Nucl. Phys. **B885**, 542 (2014).

[23] S. Kanemura, K. Nishiwaki, H. Okada, Y. Orikasa, S. C. Park, and R. Watanabe, arXiv:1512.09048.

[24] S. Antusch, E. Cazzto, and O. Fischer, J. High Energy Phys. 04 (2016) 189; S. Antusch and O. Fischer, J. High Energy Phys. 05 (2015) 053; 10 (2014) 094.

[25] G. Aad *et al.* (ATLAS Collaboration), J. High Energy Phys. 06 (2012) 039; 03 (2016) 127.

[26] T. Nomura and H. Okada, Phys. Lett. B **755**, 306 (2016); arXiv:1601.04516.

[27] G. 't Hooft and M. Veltman, Nucl. Phys. **B153**, 365 (1979).

[28] D. Y. Bardin and G. Passarino, *The Standard Model in the Making: Precision Study of the Electroweak Interactions* (Clarendon Press, Oxford, 1999).

[29] J. A. M. Vermaseren, arXiv:math-ph/0010025.